Volume 7 | Number 48 | 28 December 2019 | Pages 15085–15386

Journal of Materials Chemistry C

Materials for optical, magnetic and electronic devices

rsc.li/materials-c

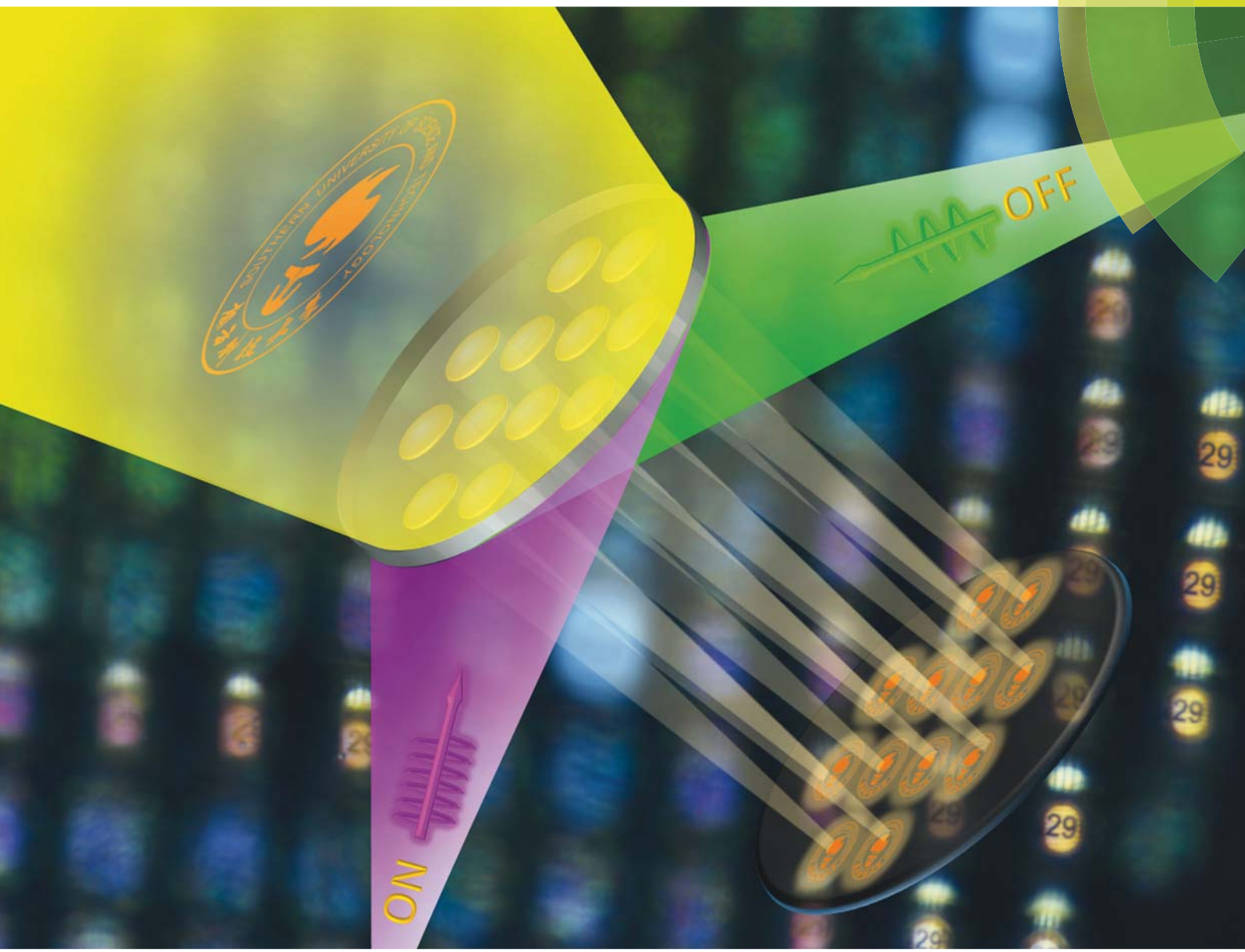

ISSN 2050-7526

ROYAL SOCIETY OF CHEMISTRY | Celebrating IYPT 2019

PAPER

Dan Luo *et al.*

A photo-switchable and photo-tunable microlens based on chiral liquid crystals

Journal of
Materials Chemistry C

PAPER

View Article Online
View Journal | View Issue

Cite this: J. Mater. Chem. C, 2019, 7, 15166

A photo-switchable and photo-tunable microlens based on chiral liquid crystals†

Yong Li, Yanjun Liu and Dan Luo *

Received 3rd September 2019,
Accepted 17th October 2019

DOI: 10.1039/c9tc04862f

rsc.li/materials-c

We demonstrate a photo-switchable and photo-tunable microlens based on chiral liquid crystals doped with an azobenzene chiral dopant immersed in water. A bi-stable microlens, which can be switched between a focusing state and scattering state through UV or green light, has been fabricated. The tuning properties of the microlens have also been demonstrated under light illumination. This bi-stable microlens possesses features including simple fabrication, low-cost, photo-switchability, and photo-tunability, and shows potential applications in dynamic imaging systems, biomimetic devices, wave-front sensors, micro-displays, light shaping *etc.*

Introduction

A liquid crystal (LC) microlens array with tunable focus length has attracted significant attention as an active optical component[1] for various applications such as imaging of microscopy systems,[2–4] beam steering,[5,6] infrared sensors,[7] wavefront modulation,[8] and THz lens.[9] Several approaches have been developed to fabricate LC microlens such as curved electrodes,[10] patterned electrodes,[11,12] laser-direct writing,[13] and nano-imprinting.[14] Different liquid crystal materials have also been applied in microlens including polymer network liquid crystals,[15] blue phase liquid crystals,[16] ferroelectric liquid crystals[17] and so on. In addition, the electrical field and temperature are usually utilized as the tuning method for LC microlens to achieve a tunable focus length,[18–21] where the electrical tunability is the most important tuning mechanism for practical applications.

Recently, a spontaneous Pancharatnam-type phase microlens array based on chiral nematic liquid crystals has been reported,[22] which provides a simple fabrication way compared to the aforementioned methods and shows potential applications in various optical sensors. However, the tunable properties of the Pancharatnam-type phase liquid crystals microlens are far from fully explored. Herein, we demonstrate a photo-switchable and photo-tunable microlens based on suspended chiral liquid crystals (CLC) doped with an azobenzene chiral dopant dispersed in water. A bi-stable microlens, which can be switched between a focusing state and a scattering state through ultra violet (UV) or green light, has been experimentally demonstrated. The tuning properties of the microlens have also been demonstrated under light illumination. This bi-stable microlens possesses features including simple fabrication, low-cost, photo-switchability, and photo-tunability, and shows potential applications in dynamic imaging systems and adaptive optics.

Experimental

The LC mixture used in our experiment consisted of a nematic liquid crystal (5CB, 87 wt%, from BaYiSpace), a chiral dopant (CB15, 8 wt%, from BaYi Space), and an azobenzene chiral dopant (Chad-3c-r, 5 wt%, from Beam.Co). Fig. 1a shows the

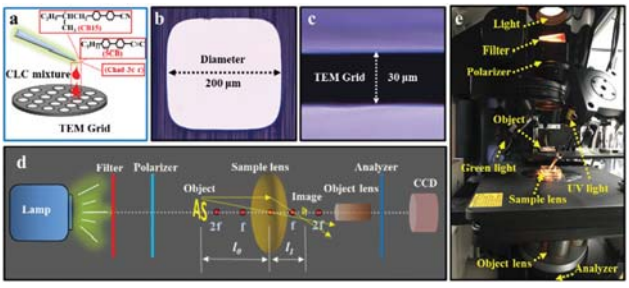

Fig. 1 (a) Schematic of the fabrication process of the microlens based on s CLC mixture (consists of CB15, 5CB and Chad-3c-r) and TEM grid. The microlens was formed by dropping the CLC mixture onto the circle-like duplex copper mesh of the TEM grid. (b) The diameter of the cooper mesh was 200 μm. (c) The thickness of the TEM grid was 30 μm. (d) The optical setup of the microlens observation and detection system, which consists of a lamp, color filter, polarizer, object, sample lens, objective lens, analyzer, and CCD. f, l_0 and l_1 represent the focal length of the microlens, object distance, and image distance, respectively. (e) Photograph of the experimental setup based on an inverted Nikon Ti microscope. An UV light source and a green light source were employed for photo-switching and photo-tuning suspended CLC microlens.

Department of Electrical & Electronic Engineering, Southern University of Science and Technology, Xueyuan Road 1088, Nanshan District, Shenzhen, Guangdong, 518055, China. E-mail: luod@sustech.edu.cn

† Electronic supplementary information (ESI) available: The videos of a photo-switchable and photo-tunable microlens. See DOI: 10.1039/c9tc04862f

schematic of the fabrication process of the microlens based on a CLC mixture and TEM grid, where the diameter (Fig. 1b) and thickness (Fig. 1c) of the circle-like duplex copper mesh of the TEM grid was 200 μm and 30 μm, respectively.

In the microlens fabrication process, a small amount of CLC mixture was firstly dropped onto the copper mesh of the TEM grid using a pipette. Then, the TEM grid with the CLC mixture was fully immersed in water, where both the bottom and top surfaces of CLC contacted with water, leading to a planar alignment of CLC configuration. The interfacial tension between water and liquid crystal droplets leads to a parallel alignment of the liquid crystal molecule on the interface, finally resulting in a spontaneously formed planar CLC configuration.[22] In this case, the LC directors in the plane of the suspended CLCs with an azimuthal angle spatially varies along the radial direction. Under the interaction of anchoring force, twisting force and tension, the suspended CLCs in the grid spontaneously formed a converging spherical microlens, where Newton rings can be clearly observed within the lens under light irradiation.[22]

Fig. 1d depicts the optical setup of microlens observation and detection, which consists of a light source lamp, color filter, polarizer, object, sample lens, objective lens, analyzer, and charge-coupled device (CCD). The white light from the lamp passed through a filter and a polarizer, and illuminated an object of letter ''AS''. Then the light passed through the sample lens and imaged after the microlens. The objective lens, the analyzer and the CCD were used to form an imaging system for image observation. It should be noticed that due to the green and ultraviolet light used for photo-switching and photo-tuning in the following experiment, a red color filter is used to filter the light from the interference. Here, f, l_0 and l_1 represent the focal length of the microlens, object distance, and image distance, respectively. The height of object letter ''AS'' was 2.07 mm, and the object distance l_0 was 17.00 mm. The inverted image was captured at l_1 = 1.30 mm with a maximum of 0.15 mm. The magnification of this microlens was calculated to be $M = l_1/l_0 = 1.3/17 \approx 0.08$, which was consistent with the apparent magnification of $M' = 0.15/2.07 \approx 0.072$ based on the ratio of image and object sizes. The tiny mismatch was due to experimental error. The focal length of the geometric lens with the object and image immersed in water was estimated to be $f = l_1 \times l_0/(l_1 + l_0) = 1.20$ mm. Fig. 1e shows the photo of the experimental setup, which is based on an inverted microscope (Nikon, Ti). An UV light (UVEC-4II, LOTS) source and a green light (LTS-ACC350-1M, LOTS) source were employed for photo-switching and photo-tuning suspended CLC microlens.

Results and discussion

Fig. 2a–c depict the schematic of the cross sectional profile of a CLC microlens in a two-dimensional (2D) grid structure, the planar state (P state), and the focal conic state (FC state). In our experiment, a convex lens (P state) was prepared in a copper mesh using a CLC doped with an azobenzene chiral dopant (ACD). The water surface provides planar alignment where the

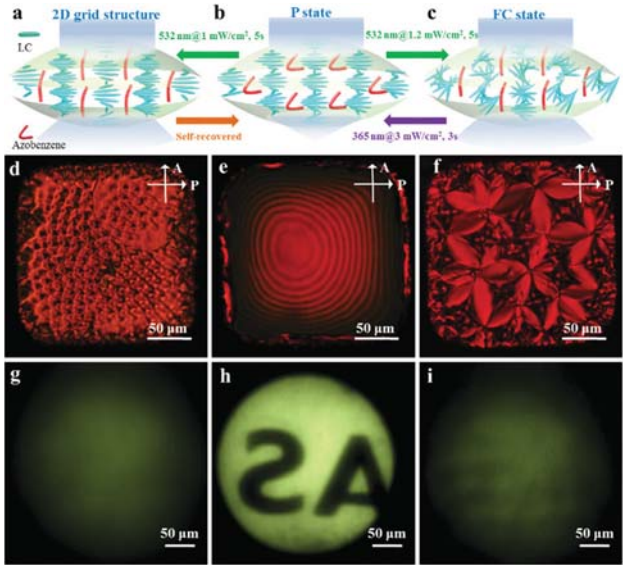

Fig. 2 Schematic of the cross sectional profile of a CLC microlens in (a) a two-dimensional (2D) grid structure, (b) the planar state (P state), and (c) the focal conic state (FC state). The lens is photo-switchable by green light or UV light between the P state and the 2D grid structure, or between the P state and the FC state, depending on different conditions, where the microlens is un-stable in the 2D grid structure but stable in the FC state. POM photo of the CLC microlens in (d) a 2D grid structure, (e) the P state, and (f) the FC state, respectively. The corresponding image from the microlens in (g) a 2D grid structure, (h) the P state, and (i) the FC state. The scale bar is 50 μm.

helical axis is perpendicular to the water/LC interface and the LC molecules are perpendicularly aligned in a copper mesh wall, resulting in a micro lens with a double convex shape (P state, as shown in Fig. 2b).[22] When the CLC microlens was in the P state, the light would pass through the lens without scattering, acting as a focusing function. The produced microlens not only has the characteristics of a geometric lens but also a Pancharatnam Berry (PB) lens.[22–24] Unlike the traditional dynamic phase produced *via* optical path difference, the PB phase corresponds to the phase shift introduced by the changes in other light wave parameters.[25] In this CLC microlens, the phase shift occurred in the plane of the suspended CLCs along the radial direction.

When illuminated with green light (532 nm), the ACD doped CLC microlens in the P state can be switched to a 2D grid structure (Fig. 2a) or FC state (Fig. 2c), depending on the intensity of green light. The state change of the microlens was due to the change of ACD from the *cis* to *trans* state that was accompanied by an increase of helical twisting power (HTP). In our experiment, the microlens was switched to a 2D grid structure (FC state) at 1 mW cm^{-2} (1.2 mW cm^{-2}) for 5 seconds upon irradiation with green light at 532 nm. The irradiation threshold for forming a 2D grid structure was measured to be 0.8 mW cm^{-2}. In the 2D grid structure case, during green light illumination, the pitch of the CLC becomes smaller, and the spatial inhomogeneity of the pitch leads to a 2D grid structure of defects. Then the disclination lines will appear between the adjacent CLCs with two different pitches,

resulting in the formation of a 2D grid structure. The POM photo of the microlens and the resulting image in the 2D grid structure is shown in Fig. 2d and g, respectively. It can be seen that, when the microlens was switched from the P state (the POM photo in the P state is shown in Fig. 2e) to the 2D grid structure, the corresponding image was switched from clear (as shown in Fig. 2h) to blurred (Fig. 2g), indicating a switchable microlens under green light. However, it was noticed that the texture of the CLC molecules in the 2D grid structure is not stable and it will spontaneously self-recover to the P state when green light is turned off.

When the intensity of green light was increased to 1.2 mW cm^{-2}, the disclination lines within the lens were denser and disordered due to the large rate of change in the pitch of the CLC. The CLC texture was finally maintained as a focal conic texture under short pitch conditions. The microlens was switched to the FC state instead. Fig. 2f and i shows the POM photo of the microlens in the FC state and the corresponding image, respectively. The POM photo of the FC state showed a typical focal conic texture of CLC, which was quite different from the 2D grid structure. The FC state obtained here was stable with unchanged structure for at least 24 hours. The CLC is stable in the FC state, due to the shorter pitch that leads to a more stable CLC texture.[26] Since the optical axis was randomly distributed when the arrangement of CLC was in the 2D grid structure or focal conic texture, the light was scattered when passing through the lens, making the lens non-imageable. The obtained image was also blurred, indicating a bi-stable switchable microlens between the P state and the FC state.

The microlens in the FC state can be photo-switched back from the FC state to the P state by ultra violet (UV) light illumination at 365 nm in 3 mW cm^{-2} for 3 seconds. When the ACD was irradiated with UV light, the HTP of the ACD decreased and the ACD changed from the *trans* to *cis* state. The illumination and photo-switching process from the FC to P state by UV light is demonstrated in the ESI,† Video S1. Therefore, the fabricated CLC microlens is photo-switchable between focusing (P state) and scattering (FC state), which can be used in a wide range of applications such as active optical components in optical microscopy, beam steering, infrared sensors, wavefront modulation and THz lens.

Besides switchability, the focal length of the CLC microlens can also be tuned by illumination with green light or UV with weak intensity, *e.g.* 0.14 mW cm^{-2} for 532 nm green light or 0.4 mW cm^{-2} for 365 nm UV light, within the P state, leading to a reversely tunable CLC microlens. It is reported that the height h of the formed biconvex lens can be determined using the formula $h \approx 3\pi^2 K_{22} aD/[\gamma p^2(\pi + 6)]$, which depends on the twist elastic constant of liquid crystals K_{22}, the helical pitch p, the interfacial tension γ, and the size of the grid a.[22] The increase (decrease) of h leads to a decrease (increase) of the radius of curvature of the convex, thus leading to a decrease (increase) of focal length f. The helical pitch can be influenced using the formula $p = 1/(\mathrm{HTP} \times C)$, where C is the dopant concentration of the chiral dopant in liquid crystals and the HTP is tunable under light illumination.[27] Under weak UV light or green light, the HTP will decrease or increase respectively.[28–30]

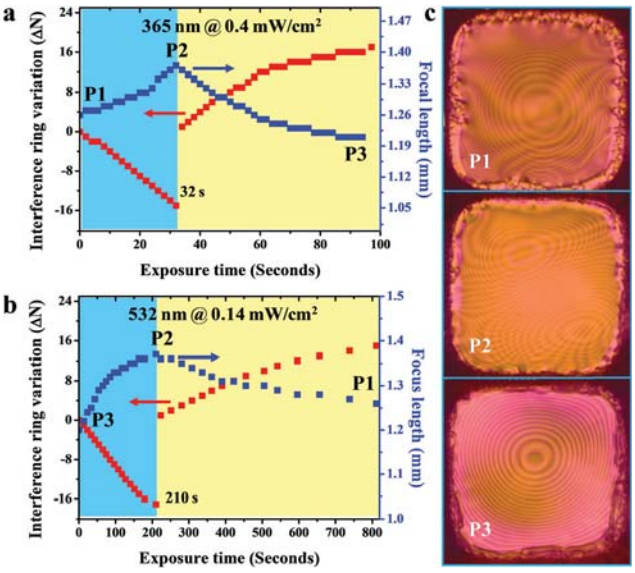

Fig. 3 Tuning the kinetic behaviour of photoresponsive microlens, with the shift of interference rings and change of focal length of the microlens during illumination of (a) 356 nm UV light at 0.4 mW cm^{-2} and (b) 532 nm green light at 0.14 mW cm^{-2}. The microlens is initially illuminated to saturate with weak green light and UV light in (a) and (b), respectively. (c) The POM photographs of P1, P2 and P3.

The tuning kinetic behaviour is quite important in photoresponsive liquid crystal materials and devices. Here, in order to see more clearly the structural change of the microlens under light illumination, weak UV and green light were used in our experiments. Fig. 3a demonstrates the shift of experimentally observed interference rings and change of the corresponding focal length in illumination with 365 nm UV light at 0.4 mW cm^{-2}, where the microlens is initially saturated with weak green light in the P state. It can be seen that the process of shift of the interference ring and change of focal length is divided into two phases that are marked by blue and yellow respectively. In the first phase (from P1 to P2, in blue region) marked by blue color, when the UV light illuminated from 0–32 s, the interference rings moved inward with a reduced number from 0 to −15, and the focal length was increased from 1.26 mm to 1.37 mm. In contrast, when the UV light was further illuminated beyond 32 s to 98 s as shown in the second phase (from P2 to P3, in the yellow region), the interference rings and focal length changed in the opposite direction. The interference rings moved outward with an increased number from 0 to 17, and the focal length was reduced from 1.37 mm to 1.20 mm.

Fig. 3b demonstrates the shift of the experimentally observed interference rings and change of the corresponding focal length under illumination with 352 nm green light at 0.14 mW cm^{-2}, where the microlens is initially in the P3 state. The focal length was firstly increased from 1.2 mm to 1.37 mm and then reduced to 1.26 mm, while the interference rings firstly moved inward and reduced by 17 and then moved outward and increased by 15. The process was opposite to that shown in Fig. 3a, except that the illumination time was in the range of 0–210 s in the blue region and 210—811 s in the yellow

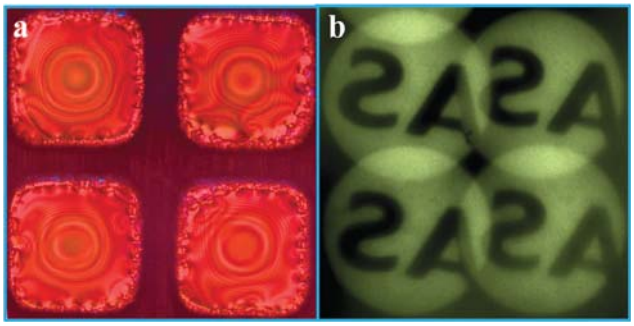

Fig. 4 (a) Photo of the 2 × 2 microlens array. (b) Images from the microlens array of letters "AS".

region under green light illumination. The POM photographs of P1, P2 and P3 are shown in Fig. 3c. Under photo illumination, the phase change of the chiral dopant leads to a change of the helical pitch p, then leads to the height h, and finally the focal length of microlens.

The dynamic video of microlens and image during the tuning process under green light illumination is shown in the ESI,† Video S2. This phenomenon (increase and then decrease of focal length) is most likely due to the fact that the value of h is not only determined by the pitch (p) but also the twist elastic constant K_{22} and the interfacial tension γ. The elastic energy of the liquid crystal and the surface tension between the liquid crystal and the water may also influence the value of h. The resulting process is quite complicated and the physical mechanism behind it is not fully explained yet, which will be investigated in our future work.

The photo of the CLC 2 × 2 microlens array and the corresponding images are shown in Fig. 4a and b, respectively. The height of object letter "AS" was 2.07 mm, and the object distance l_0 was 17.00 mm. The inverted image was captured at l_1 = 1.30 mm with a height of 0.15 mm. The magnification of this microlens was calculated to be $M = l_1/l_0 = 1.3/17 \approx 0.08$, which was consistent with the apparent magnification of $M' = 0.15/2.07 \approx 0.072$ based on the ratio of the image and object sizes. The tiny mismatch was due to experiment measurement error. The focal length of the geometric lens with the object and image immersed in water was estimated to be $f = l_1 \times l_0/(l_1 + l_0) = 1.20$ mm. The microlens array with an extremely large field of view angles, low aberration and distortion, high temporal resolution and infinite depth of field show great potential for applications such as 3D displays, photolithography, imaging, optical communications and flat panel displays. The bistable microlens possesses features such as photo-switchability and photo-tunability, demonstrating great application potential as active optical components in optical microscopy, beam steering, infrared sensors, wavefront modulation and THz lens.

Conclusions

In summary, a photo-switchable and photo-tunable microlens based on chiral liquid crystals doped with an azobenzene chiral dopant has been experimentally demonstrated. A bi-stable microlens, which can be switched between a focusing state and a scattering state through UV or green light, has been experimentally demonstrated. The tuning properties of the microlens have also been demonstrated under light illumination. This bi-stable microlens possesses features including simple fabrication, low-cost, photo-switchability, and photo-tunability, and shows potential applications in 3D imaging systems and optical communications, compound photonic devices *etc.*

Conflicts of interest

There are no conflicts to declare.

Acknowledgements

This work is supported by Natural National Science Foundation of China (NSFC) (61875081); Shenzhen Science and Technology Innovation Commission (JCYJ20180305180700747).

References

1 Y. H. Lin, Y. J. Wang and V. Reshetnyak, *Liq. Cryst. Rev.*, 2017, **5**, 111.
2 A. Orth and K. Crozier, *Opt. Express*, 2012, **20**, 13522.
3 P.-Y. Hsieh, P.-Y. Chou, H.-A. Lin, C.-Y. Chu, C.-T. Huang, C.-H. Chen, Z. Qin, M. M. Corral, B. Javidi and Y.-P. Huang, *Opt. Express*, 2018, **26**, 10981.
4 Z. Xin, D. Wei, X. Xie, M. Chen, X. Zhang, J. Liao, H. Wang and C. Xie, *Opt. Express*, 2018, **26**, 4035.
5 S. Masuda, S. Takahashi, T. Nose, S. Sato and H. Ito, *Appl. Opt.*, 1997, **36**, 4772.
6 A. Akatay, C. Ataman and H. Urey, *Opt. Lett.*, 2006, **31**, 2861.
7 Z. Xin., D. Wei., M. Chen, C. Hu, J. Li, X. Zhang, J. Liao, H. Wang and C. Xie, *Opt. Mater. Express*, 2019, **9**, 183.
8 L. Hu, L. Xuan, D. Li, Z. Cao, Q. Mu, Y. Liu, Z. Peng and X. Lu, *J. Opt. A: Pure Appl. Opt.*, 2009, **11**, 015511.
9 Z. Shen, S. Zhou, S. Ge, W. Duan, L. Ma, Y. Lu and W. Hu, *Opt. Express*, 2019, **27**, 8800.
10 Y.-H. Fan, H. Ren, X. Liang, H. Wang and S.-T. Wu, *J. Disp. Technol.*, 2005, **1**, 151.
11 T. Nose and S. A. Sato, *Liq. Cryst.*, 1989, **5**, 1425.
12 J. F. Algorri, N. Bennis, V. Urruchi, P. Morawiak, J. M. Sánchez-Pena and L. R. Jaroszewicz, *Sci. Rep.*, 2017, **7**, 17318.
13 Z. He, Y.-H. Lee, R. Chen, D. Chanda and S.-T. Wu, *Opt. Express*, 2018, **26**, 21184.
14 Z. He, Y.-H. Lee, R. Chen, D. Chanda and S.-T. Wu, *Opt. Lett.*, 2018, **43**, 5062.
15 H. Ren, Y.-H. Fan, S. Gauza and S.-T. Wu, *Opt. Commun.*, 2004, **230**, 267.
16 S.-H. Lin, L.-S. Huang, C.-H. Lin and C.-T. Kuo, *Appl. Phys. Lett.*, 2010, **96**, 113505.
17 Y. Ma, A. M. W. Tam, X. T. Gan, L. Y. Shi, A. K. Srivastava, V. G. Chigrinov, H. S. Kwok and J. L. Zhao, *Opt. Express*, 2019, **27**, 10079.

18 H. C. Lin and Y. H. Lin, *Appl. Phys. Lett.*, 2011, **98**, 083503.
19 J. Beeckman, T. H. Yang, I. Nys, J. P. George, T. H. Lin and K. Neyts, *Opt. Lett.*, 2018, **43**, 271.
20 J. H. Kim, Y. H. Kim, H. S. Jeong, M. Srinivasarao, S. D. Hudson and H. T. Jung, *RSC Adv.*, 2012, **2**, 6729.
21 K. C. Heo, S. H. Yu, J. H. Kwon and J. S. Gwag, *Appl. Opt.*, 2013, **52**, 8460.
22 P. Popov, L. W. Honaker, M. Mirheydari, E. K. Mann and A. Jakli, *Sci. Rep.*, 2017, **7**, 1603.
23 Y. Bouligand, *Tissue Cell*, 1972, **4**, 189.
24 K. Gao, H. H. Cheng, A. K. Bhowmik and P. J. Bos, *Opt. Express*, 2015, **23**, 26086.
25 Z. He, Y. H. Lee, R. Chen, D. Chanda and S. T. Wu, *Opt. Lett.*, 2018, **43**, 5062.
26 W. Greubel, *Phys. Lett.*, 1974, **25**, 5.
27 G. S. Chilaya and L. N. Lisetski, *Mol. Cryst. Liq. Cryst.*, 1986, **140**, 243.
28 L. Zhang, M. Wang, L. Wang, D.-K. Yang, H. Yu and H. Yang, *Liq. Cryst.*, 2016, **43**, 750.
29 J. Sun, L. Yu, L. Wang, C. Li, Z. Yang, W. He, C. Zhang, L. Zhang, J. Xiao, X. Yuan, F. Li and H. Yang, *J. Mater. Chem. C*, 2017, **5**, 3678.
30 J. Sun, R. Lan, Y. Gao, M. Wang, W. Zhang, L. Wang, L. Zhang, Z. Yang and H. Yang, *Adv. Sci.*, 2018, **5**, 1700613.